RSC Advances

PAPER

View Article Online
View Journal | View Issue

Cite this: *RSC Adv.*, 2026, **16**, 16586

Fabrication of high-strength and self-healing polyurethane composites *via* Diels–Alder dynamic bonds for sustainable thermal management materials

Zhangyong Yu * and Zhaokun Yang

Electronic devices generate a large amount of heat, which can damage devices if not dissipated in a timely manner. Thermal interface materials (TIMs), which are used to enhance heat dissipation efficiency, face challenges in simultaneously achieving high thermal conductivity, desired mechanical properties, and remarkable adhesive, self-healing and recycle properties. In this work, we successfully synthesized a series of dynamically reversible polyurethane (DRPU) elastomers *via* a Diels–Alder (DA) reaction to serve as TIM matrices. DRPUs demonstrated excellent mechanical properties, with a tensile strength of 35.8 MPa, an elongation at break of 714% and a toughness of 146.07 MJ m^{-3}. Owing to the synergistic effects of dynamic covalent interactions and strong intrinsic cohesion, DRPUs exhibited a good lap-shear strength of 3.3 MPa on aluminum plates. Additionally, DRPUs displayed efficient self-healing properties, with a self-healing efficiency of 87% that remained at 78% after multiple healing cycles. Furthermore, pre-prepared polydopamine-modified Al_2O_3(f-Al_2O_3) was confirmed to increase the thermal conductivity of DRPUs.

Received 29th January 2026
Accepted 28th February 2026

DOI: 10.1039/d6ra00787b

rsc.li/rsc-advances

1 Introduction

Electronic devices have achieved unprecedented development in the direction of miniaturization, integration and precision with the arrival of the 5G era.[1] As the power density of electronic devices continues to increase, it is difficult to dissipate large amounts of heat promptly, especially in the presence of a polymer matrix packaging or protection. This heat accumulation results in substantial performance degradation in electronic devices.[2] Traditionally, heat-dissipating components have helped remove this substantial heat, but the low-conductive air layers between heat-generating and heat-dissipating components hinder heat transmission.[3] Therefore, thermal interface materials (TIMs) are employed to fill these air layers to improve heat dissipation efficiency.[4,5]

Polymer composites, such as TIMs, have been widely utilized for thermal management because of their lightweight, low cost, high comprehensive performance and easy processability.[6,7] Due to the complexity of service environments, advanced TIMs must meet several performance requirements,[8,9] including adequate mechanical properties to prevent component collisions, strong adhesive strength to eliminate the excess air between interfaces and enhance heat transfer, and excellent self-healing property to maintain the stability of performances and prolong the service life.[10,11]

Polyurethanes (PUs) are ideal polymer matrices for adhesive-type TIMs due to their inherent flexibility, tunable mechanical properties, and strong adhesion.[12–14] However, traditional PU-based TIMs lack self-healing property, which is crucial for long-term performance reliability. To address this limitation, the incorporation of reversible covalent bonds,[15] including imine bonds,[16] boronic ester bonds,[17] disulfide bonds[18] and Diels–Alder (DA) covalent adducts,[19] into PU matrices has been proposed as an effective strategy. Wu *et al.*[20] synthesized a robust and self-healing poly(urethane-urea-imide) (PUUI) elastomer as an exemplary TIM candidate. PUUI exhibited a self-healing efficiency of 94%, which can be attributed its hydrogen bonds and disulfide bonds. Diels–Alder (DA) covalent adducts between maleimide and furan moieties emerge as particularly promising candidates[21–23] as they exhibit thermal reversibility, forming stable adducts at lower temperatures and undergoing retro-DA dissociation at high temperatures.[24] Meanwhile, the cyclic structure formed through the DA reaction helps maintain the mechanical strength and enhance the thermal conductivity of the PU matrix due to its phonon transport.[25,26] In addition, typical PUs show low thermal conductivities of 0.1–0.2 W m^{-1} K^{-1}, which hinder effective dissipation of the heat generated by operating devices.[6] The thermal conductivity of composite materials can be improved by the incorporation of inorganic fillers,[27] such as carbon

School of Mechanical Technology, Wuxi University of Technology, Wuxi 214121, China. E-mail: 13771176151@163.com; Tel: +86-510-81838868

nanotubes (CNTs), graphene,[28,29] alumina oxide (Al_2O_3)[30] and boron nitride (BN).[31,32] CNTs and graphene exhibit both high thermal conductivity (2000–3000 W m^{-1} K^{-1}) and electrical conductivity, thus limiting their use in TIMs for electronic devices. Boron nitride (BN), a 2D-layered material with a hexagonal crystal structure, exhibits a high thermal conductivity; however, it suffers from harsh preparation conditions and high production costs. Aluminum oxide (Al_2O_3) is a low-cost compound with intrinsic thermal conductivity, making it a promising filler for polymer matrices in industrial applications.

Herein, we synthesized a series of robust and self-healing dynamically reversible polyurethanes (DRPUs) by incorporating a pre-prepared Diels–Alder (DA) covalent adduct-based diol (DABF) as a chain extender into the prepolymer. DABF was prepared *via* the Diels–Alder reaction between *N*,*N*′-(4,4′-diphenylmethane)bismaleimide (BMI) and furfuryl alcohol (FA). The high electron deficiency of the maleimide double bond, induced by the aromatic *N*-substituted unit in BMI, significantly enhanced its reactivity with bio-based FA.[33] Additionally, the double benzene ring structure of BMI improved the rigidity of DABF and, consequently, the DRPU matrix. DRPU exhibited remarkable mechanical properties, including a high elongation at break (714%), tensile strength (35.8 MPa) and toughness (146.1 MJ m^{-3}). Notably, it also demonstrated efficient self-healing behavior at a mild temperature of 65 °C, with a self-healing efficiency of 89% after 24 h. Furthermore, dopamine-modified Al_2O_3 fillers (f-Al_2O_3), which could improve the compatibility between Al_2O_3 and the DRPU matrix, were incorporated into DRPU to prepare DRPU/f-Al_2O_3 TIMs with increased thermal conductivity.

2 Results and discussion

2.1 Synthesis of DRPUs

The synthetic route for DRPUs is illustrated in Fig. 1a. Long chain PTMEG was selected as the soft segment, while IPDI and DABF were employed as hard segments. A three-dimensional network structure was formed through crosslinking by TEA (the molar ratios are listed in Table S1). Due to the incorporation of DA dynamic bonds, the damaged regions of DRPUs could be self-healed, further extending their service life. Meanwhile, moderate crosslinking induced by TEA not only enhanced the tensile strength but also improved the solvent resistance of DRPUs.

The structures of DRPUs were characterized by FT-IR spectroscopy. As shown in Fig. 1b, using $DRPU_{0.52}$ as a representative example, the characteristic peak at 2238 cm^{-1} is assigned to the N=C=O stretching vibrations, and the area of this peak decreased in prepolymer and disappeared in $DRPU_{0.52}$. To quantitatively monitor the reaction progress, we conducted acetone-di-*n*-butylamine titration and determined the residual isocyanate content, which confirmed that water molecules did not influence the reaction and the crosslinking reaction proceeded successfully. The peaks at 3329 cm^{-1} and 1710 cm^{-1} are attributed to the N–H and C=O stretching vibrations, respectively. A distinct peak at 1511 cm^{-1} (Fig. S2) is assigned to the C=C stretching vibration of the aromatic ring in the DA adduct formed by BMI and FA, and this peak appeared only in the DRPU samples after the introduction of DABF (DA adduct diol)[21,23] and is absent in the prepolymer without DABF (Fig. 1b). The peak at 1775 cm^{-1} is assigned to the C=O stretching vibration of the succinimide ring in the DA adduct (Fig. S2),

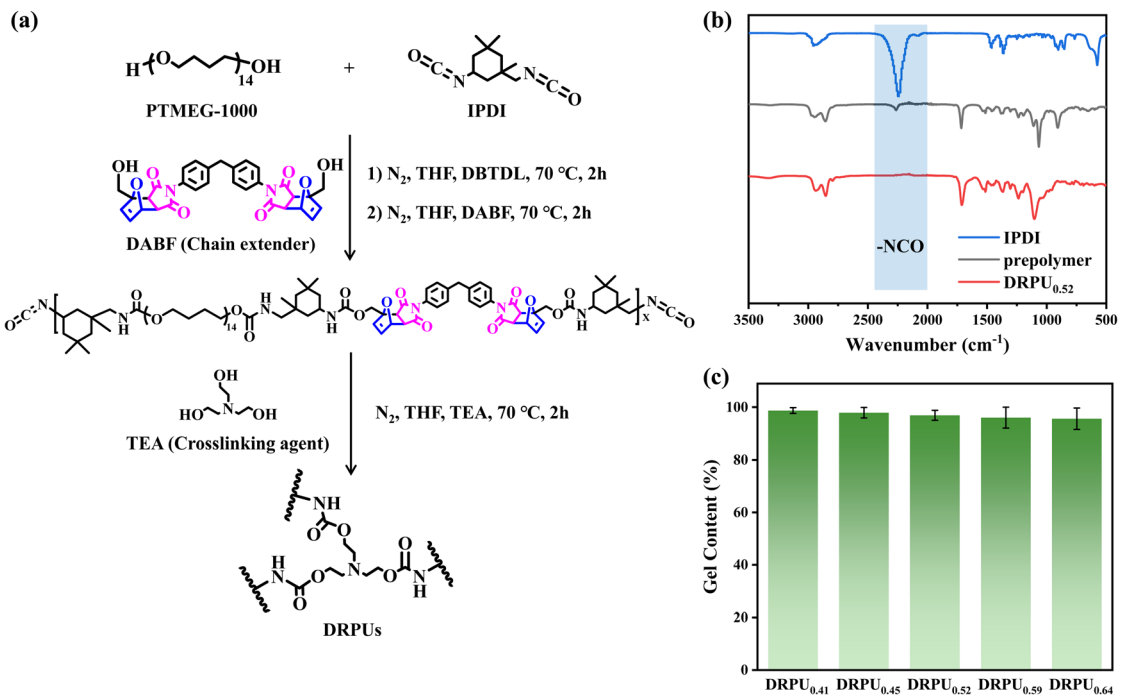

Fig. 1 (a) Synthetic route of DRPUs. (b) FT-IR spectra of IPDI, prepolymer and $DRPU_{0.52}$. (c) Gel content of DRPUs in hot ethanol.

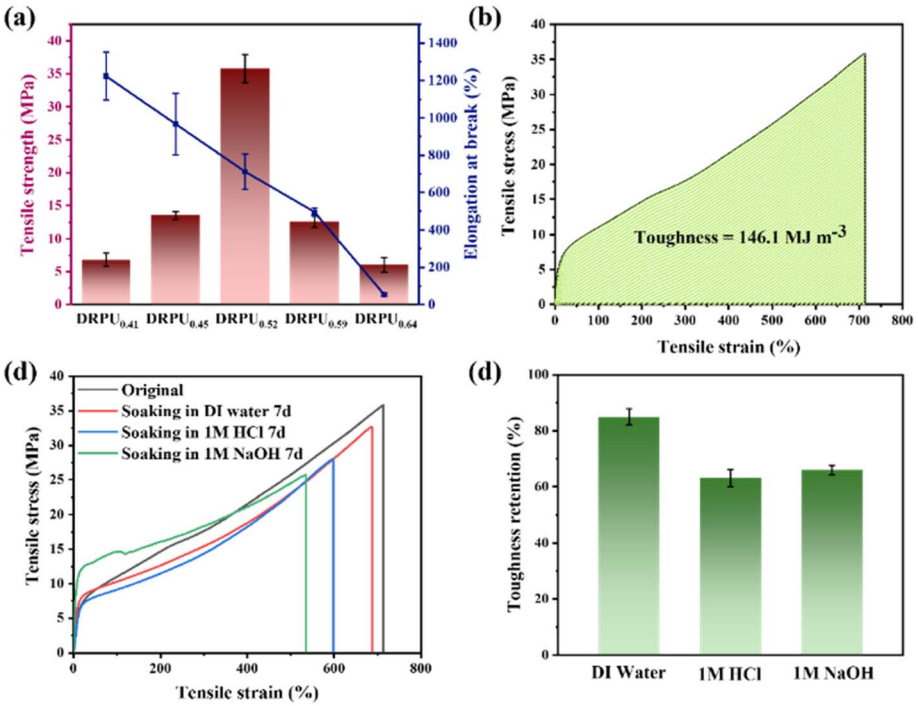

Fig. 2 (a) DSC curves of DRPUs. (b) DMA curves of $DRPU_{0.52}$. (c) TGA and (d) DTG curves of DRPUs.

which is the characteristic absorption peak of the DA adduct formed by maleimide (BMI) and furan (FA),[23,33] verifying the successful incorporation of DA bonds. All the results confirmed the successful preparation of DRPUs.

Since the reactivity of terminal hydroxyl groups in DABF was much lower than that in PTMEG, to verify the complete reaction of DABF, we evaluated the gel content of DRPUs after extracting it in hot ethanol (Fig. 1c). A gradual decrease in gel content was observed from 98.2% to 95.6% with an increase in the hard-segment-content, and all DRPUs maintained their gel content above 95%. Results confirmed that only a trace amount of unreacted DABF was dissolved in hot ethanol. Furthermore, we tested the water resistance of DRPUs (Fig. S3). The water absorption rate of DRPUs slightly decreased from 8.53% to 2.05% with an increase in the hard-segment-content. This trend could be attributed to the water absorption property of the PTMEG segments.

2.2 Thermal properties of DRPUs

The thermal performances of DRPUs were evaluated by DSC, DMA and TGA. As shown in Fig. 2a, the glass transition temperature (T_g) of DRPUs increased from −57.03 °C to −50.88 °C with an increase in the hard-segment-content, attributed to the enhanced molecular chain rigidity. From Fig. 2b, $DRPU_{0.52}$ demonstrated an elastic solid behavior across the tested temperature range (−80 °C to 70 °C), with storage modulus (G') decreasing from 1.17×10^4 Pa to 39.16 Pa and loss modulus (G'') decreasing from 3.93×10^2 Pa to 12.47 Pa. The storage modulus was always higher than the loss modulus. From Fig. 2c and d, 5% mass decomposition temperature ($T_{d,5\%}$) of DRPUs was above 180 °C, which could meet the temperature requirements of vehicle-mounted devices. The thermal decomposition could be divided into three processes. Initially, most of the hard segments underwent thermal decomposition below 260 °C, and then, soft segments decomposed between 290 °C and 380 °C. Finally, BMI segments decomposed between 380 °C and 600 °C.

2.3 Mechanical properties of DRPUs

The mechanical properties of TIMs are critical factors to determine their service life. As shown in Fig. 3a, b and S4, with the increasing hard-segment-content, the tensile strength of DRPUs first increased and then decreased, while the elongation at break gradually decreased. $DRPU_{0.52}$ demonstrated optimal mechanical properties with a tensile strength of 35.8 MPa, elongation at break of 714% and toughness of 146.1 MJ m^{-3}, which were better than most of the literature-reported values (Table S3). The high mechanical properties of $DRPU_{0.52}$ could be attributed to three synergistic factors. (1) Strain-induced crystallization of PTMEG: From Fig. S5a, the original $DRPU_{0.52}$ exhibited no crystalline features under polarized light, while $DRPU_{0.52}$ demonstrated distinct strain-induced crystallization behavior along the stretching direction when stretched to produce strain (Fig. S5b–d). (2) Long molecular chain (Table S2) and (3) appropriate crosslinking imparted by TEA. However, the tensile strength of $DRPU_{0.59}$ and $DRPU_{0.64}$ decreased significantly, possibly due to two factors: (1) reduced PTMEG content, diminishing strain-induced crystallization during stretching process, and (2) the low reactivity of terminal hydroxyl groups of DABF, leading to the shortening of the molecular chain length of prepolymer (Table S2), which restricted stress dissipation through chain mobility. When applied to electronic devices,

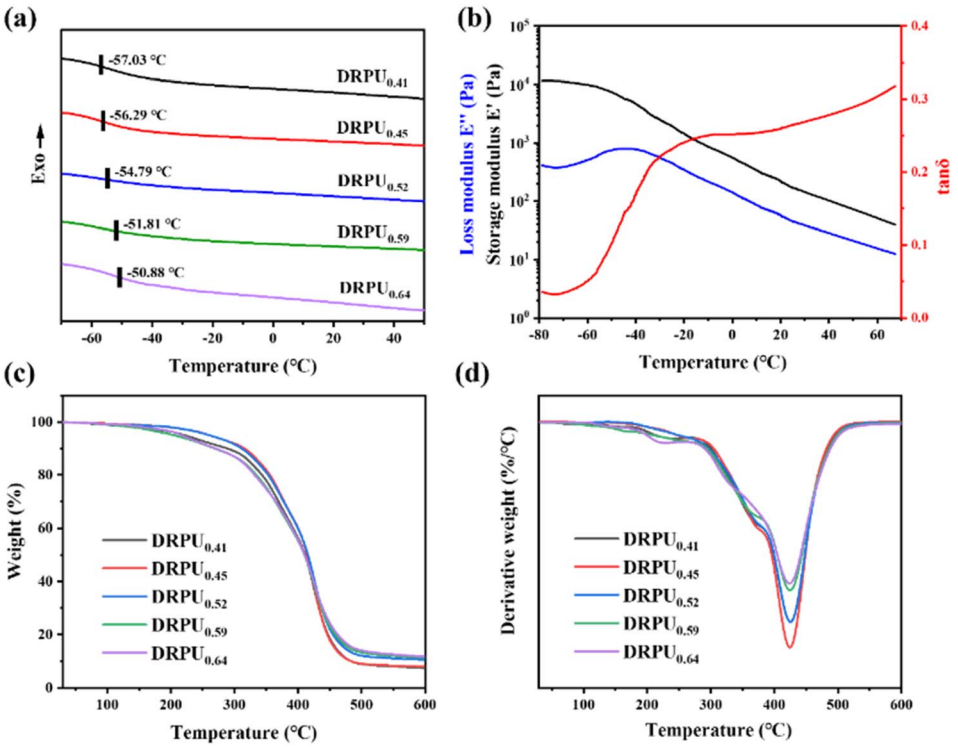

Fig. 3 (a) Tensile strength and elongation at break of DRPUs. (b) Toughness of $DRPU_{0.52}$. (c) Stress–strain curves and (d) toughness retention of $DRPU_{0.52}$ before and after soaking in DI water, 1 M HCl and 1 M NaOH solution for 7 days.

TIMs may face uncontrollable changes under environmental conditions, such as acid and base conditions. To evaluate the stability of $DRPU_{0.52}$, we immersed it in three different media, namely, acidic solution (1 M HCl), alkaline solution (1 M NaOH) and deionized water (DI) for 7 days. Visual inspection (Fig. S6) confirmed that no significant dissolution of $DRPU_{0.52}$ was observed in all three media after 7 days, and it retained toughness values of 84.9% (DI water), 63.1% (1 M HCl) and 65.9% (1 M NaOH) compared with the original sample (Fig. 3c and d). The decline in mechanical properties upon immersion in HCl and NaOH might be due to the hydrolysis of the ether and urethane bonds. Although the mechanical properties of $DRPU_{0.52}$ immersed in HCl and NaOH were lower than those of the original sample, $DRPU_{0.52}$ could still be suitable for applications in complicated environments.

2.4 Self-healing and recyclable properties of DRPU

The self-healing property of $DRPU_{0.52}$ (as an example) was evaluated through scratch tests. The self-healing process consisted of two stages: $DRPU_{0.52}$ was first heated at 110 °C for 10 min and self-healed at 65 °C for several hours. The scratched region quickly disappeared within 10 min, as observed using a polarized optical microscope (Fig. S7a–c). With the extension of healing time, as shown in Fig. 4a, both the tensile strength and elongation at break of the self-healed $DRPU_{0.52}$ exhibited progressive increments. The self-healing efficiency (toughness after healing/original × 100) of $DRPU_{0.52}$ was 51% after healing for 12 h (Fig. S8a). Remarkably, extending the healing time to 24 h, $DRPU_{0.52}$ achieved a recovered toughness of 127.1 MJ m^{-3}, corresponding to an impressive self-healing efficiency of 87%. To further investigate the repeatability of the self-healing process, the self-healed $DRPU_{0.52}$ was cut again at the same position for the second self-healing, followed by the third. As shown in Fig. 4b, $DRPU_{0.52}$ maintained excellent self-healing property through multiple cycles, demonstrating healing efficiencies of 85% and 78% for the 2nd and 3rd cycles, respectively (Fig. S8b). The above results clearly indicate the outstanding and sustainable self-healing properties of $DRPU_{0.52}$.

Fig. 4c shows the self-healing mechanism of $DRPU_{0.52}$, which operates through a thermally reversible Diels–Alder (DA) reaction process. When the scratch regions are heated to 110 °C, the retro-DA reaction occurs, cleaving the long chains of $DRPU_{0.52}$ into shorter and mobile chains. These chains migrated and redistributed *via* thermal motion, effectively filling the scratch regions, while PU without DA dynamic covalent bonds failed to achieve self-healing of the scratch regions due to the limited thermal motion of its long chains (Fig. S7d–f). Subsequently, maintaining the temperature at 65 °C facilitated the reformation of long chains through the DA reaction, reconstructing the polymer network structure. The above processes enabled almost all damaged regions to be closed, thus recovering the mechanical properties.

The recyclability of $DRPU_{0.52}$ was evaluated by exploiting the DA dynamic characteristics. As shown in Fig. 4d, $DRPU_{0.52}$ was first cut into pieces and subjected to heat treatment involving hot pressing at 110 °C for 10 min, followed by warming at 65 °C for 24 h. Remarkably, the reprocessed $DRPU_{0.52}$ exhibited excellent recyclability, achieving a tensile strength of 31.8 MPa

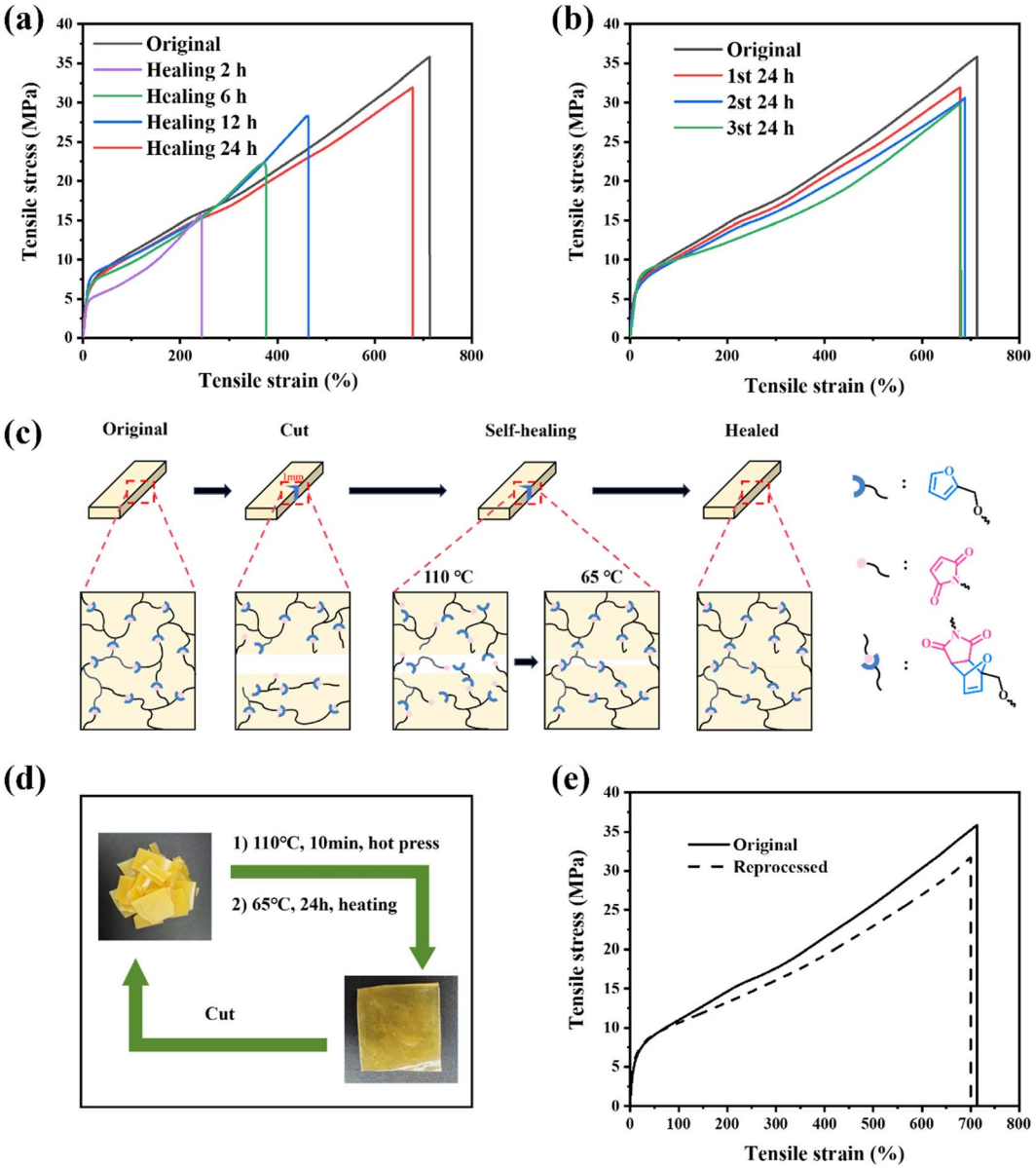

Fig. 4 Stress–strain curves of $DRPU_{0.52}$ at (a) different healing times and (b) different healing cycles. (c) Schematic of the healing process of a crack in $DRPU_{0.52}$ based on both the DA reaction and thermal movement of molecular chains. (d) Schematic of physical reprocessing. (e) Stress–strain curves of $DRPU_{0.52}$ before and after reprocessing physically.

and toughness of 127.9 MJ m^{-3}, corresponding to a reprocessing efficiency of 88% (Fig. 4e). The structure of the reprocessed $DRPU_{0.52}$ was confirmed by FT-IR spectroscopy, as shown in Fig. S9. The characteristic peak belonging to the DA bond at 1775 cm^{-1} reformed, demonstrating the reformation of the reversible DA bonds during reprocessing. The above results indicate that $DRPU_{0.52}$ could be effectively recycled *via* hot pressing.

2.5 Adhesive property of DRPUs

The adhesive property of DRPUs was evaluated through lap-shear tests using aluminum substrates. From Fig. 5a, the lap-shear strength was 3.5 MPa for $DRPU_{0.41}$ and decreased with increasing hard-segment-content, showing a clear inverse relationship between hard-segment-content and lap-shear strength. The lap-shear strength of adhesive materials is determined by the balance between the cohesion of the matrix and the interfacial adhesion between the matrix and the substrate. For DRPUs, with increasing hard-segment-content, the rigidity of DRPUs increased while the flexibility decreased. The adhesion property of the DRPU matrix to wet the aluminum substrate surface was reduced, leading to a decrease in interfacial adhesion.[20] Moreover, the excessive hard-segment aggregation increased the brittleness of the matrix, and the cohesion of the matrix decreased due to the decrease in the mobility of molecular chains. However, partial hydrogen bonds in the matrix could be dissociated upon heating and reformed at the matrix

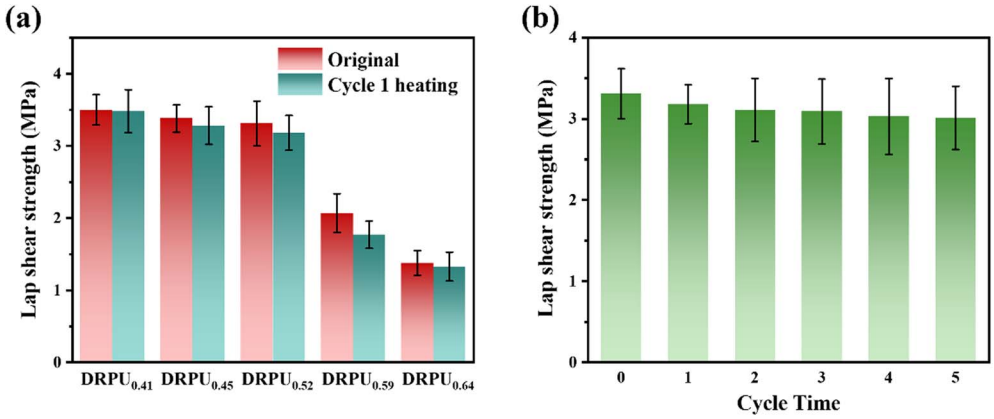

Fig. 5 (a) Original and lap-shear tests of DRPUs for one recycle. (b) Multiple recycle lap-shear tests of $DRPU_{0.52}$.

and aluminum interface, enhancing the interaction between interfaces. Thus, $DRPU_{0.52}$ exhibited the optimal balance between matrix flexibility and cohesion, thus showing the suitable lap-shear strength (3.3 MPa).

Notably, $DRPU_{0.52}$ demonstrated its potential as a reusable adhesive. The aluminum substrates could be re-bonded with $DRPU_{0.52}$ after heating $DRPU_{0.52}$ at 110 °C for 30 min, followed by curing at 65 °C for 24 h. As shown in Fig. 5b, the lap-shear strength of $DRPU_{0.52}$ remained at 3.0 MPa after five cycles, retaining over 90% of its original lap-shear strength. The remarkable reusable adhesive property of $DRPU_{0.52}$ can be attributed to its transition from elastic state to viscous state when heating, which facilitates the rewetting of the adherend surfaces. Additionally, reversible hydrogen bonds and DA bonds in the matrix make important contributions. The excellent reusable adhesive property of $DRPU_{0.52}$ could potentially result in its more cost-effective, consistent and long-lasting performance.

2.6 Thermal conductivity of $DRPU_{0.52}$/f-Al_2O_3

To improve the thermal conductivity of $DRPU_{0.52}$, we incorporated 5 μm Al_2O_3 into its matrix. Recognizing the importance of compatibility between organic matrix and inorganic fillers, Al_2O_3 fillers were first modified by polydopamine (PDA). The mechanism of Al_2O_3 modified by PDA coating is shown in Fig. 6a.[34,35] Dopamine was oxidized and self-polymerized into PDA in alkaline and oxygen-rich conditions. Then, the highly cross-linked PDA layers were bound to the Al_2O_3 surface through coordination and π–π non-covalent interactions to form PDA-coated Al_2O_3 (f_3-Al_2O_3). For comparison, phthalate coupling agent TC114 and silane coupling agent KH550 were also employed to modify the Al_2O_3 fillers, named as f_1-Al_2O_3 and f_2-Al_2O_3. From Fig. 6b and S10, TC114, KH550, and PDA were successfully modified on Al_2O_3 while maintaining the original crystalline peak positions, indicating that the modifications did not affect the crystal structure of Al_2O_3.

Fig. 6c shows the thermal conductivity of the composite material $DRPU_{0.52}$/f-Al_2O_3 with 10% f-Al_2O_3 content. $DRPU_{0.52}$/10% f_3-Al_2O_3 exhibited the highest thermal conductivity of 0.2629 W m^{-1} K^{-1}, indicating the better compatibility between its fillers and matrix compared with the other two samples with f_1-Al_2O_3 and f_2-Al_2O_3. This improved compatibility could be attributed to hydrogen bonding interactions between the catechol and amino groups on the PDA layer of f_3-Al_2O_3 and the urethane bonds in the DRPU matrix.[35] On the other hand, the benzene ring structures, both in the PDA layer and in the DABF hard segments, of the DRPU matrix formed π–π stacking interactions, which further enhanced the interfacial bonding between the filler and the matrix. As shown in Fig. 6d, with the increasing f_3-Al_2O_3 content, more thermal conductivity paths could be formed, and thus, the thermal conductivity of $DRPU_{0.52}$/f-Al_2O_3 gradually increased. The highest thermal conductivity reached 0.6329 W m^{-1} K^{-1} with 80 wt% f-Al_2O_3 content, which was 344.8% higher than that of the $DRPU_{0.52}$ matrix.

To intuitively demonstrate the potential application of $DRPU_{0.52}$/f-Al_2O_3 in thermal management materials, we recorded the surface temperature of $DRPU_{0.52}$/f_3-Al_2O_3 at different heating times using an infrared thermal imager. The samples were cut into cubes with the same size of 20 mm × 20 mm × 1 mm and then heated on a hot stage at 75 °C. The change in the surface temperature is displayed in Fig. 6e. The temperature change rate of $DRPU_{0.52}$/80% f-Al_2O_3 was significantly higher than that of the original $DRPU_{0.52}$, which took only 35 s to reach the set temperature, indicating good thermal transfer capabilities.

3 Experimental

3.1 Materials

Polytetramethylene ether glycol (PTMEG, M_n = 1000), ditin butyl dilaurate (DBTDL, 95%), *N*,*N*′-(4,4′-diphenylmethane)bismaleimide (BMI, 98%), and triethanolamine (TEA, 98%) were purchased from Sinopharm Chemical Reagent Co., Ltd (Shanghai, China). Isophorone diisocyanate (IPDI, 99%), furfuryl alcohol (FA, 98%), tetrahydrofuran (THF, 99.5%), and Al_2O_3 (5 μm, 99.9%) were purchased from Macklin Biochemical Co., Ltd (Shanghai, China). Dopamine hydrochloride (DA) was purchased from Adamas Reagent Co., Ltd (Shanghai, China).

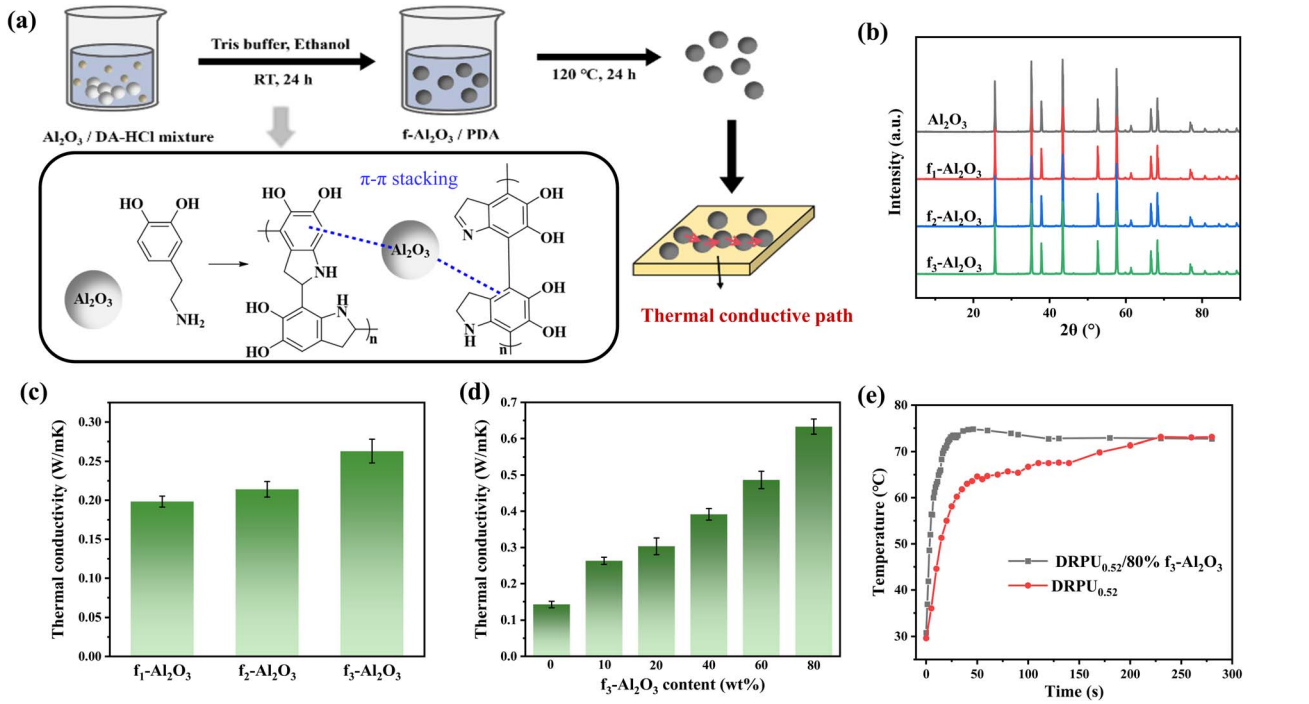

Fig. 6 (a) Schematic of the coating of Al_2O_3 by PDA. (b) X-ray diffraction (XRD) patterns of Al_2O_3 and f-Al_2O_3 under three modification methods. (c) Thermal conductivity of $DRPU_{0.52}$/10% f-Al_2O_3 under three modification methods. (d) Thermal conductivity of $DRPU_{0.52}$/f_3-Al_2O_3 with different f-Al_2O_3 contents. (e) Infrared images of $DRPU_{0.52}$ and $DRPU_{0.52}$/80% f_3-Al_2O_3 recorded after working for 280 s.

Tris buffer (0.01 mol L^{-1}, pH = 8.5) was purchased from Yuanye Bio-Technology Co., Ltd (Shanghai, China).

3.2 Synthesis of dynamically reversible polyurethanes (DRPUs)

Diols containing DA bonds (DABF) were synthesized as described in the SI. ^{1}H NMR and FT-IR spectra of DABF are shown in Fig. S1. After drying PTMEG under vacuum at 120 °C for 2 h, IPDI, PTMEG, DBTDL and THF were added into a 250 mL three-necked flask to react at 70 °C for 2 h under a nitrogen atmosphere. Then, DABF was added dropwise to the mixture and reacted at 70 °C for an additional 2 h. Afterwards, TEA was added to the prepolymer and reacted at 70 °C for 3 h. At the end of the reaction, the product was placed in a vacuum oven at room temperature to remove bubbles and then poured into a mold at 50 °C for 12 h and 80 °C for 4 h.

Following the same procedure, the fabrication of DRPUs with different molar ratios of PTMEG and DABF are listed in Table S1. The obtained products were designated as $DRPU_x$, where x is the hard segment ratio of DRPUs.

3.3 Synthesis of DRPUs/f-Al_2O_3

10 g Al_2O_3 (5 μm) was dispersed in a mixed solution of 60 mL of Tris buffer (pH = 8.5) and 20 mL of ethanol and added into a 250 mL round-bottom flask. Then, 1 g of dopamine hydrochloride was added, and the system was reacted at room temperature for 24 h. After the reaction was completed, the modified Al_2O_3 (f_3-Al_2O_3) was obtained by filtering and drying in oven at 120 °C for 12 h. f_3-Al_2O_3 was dispersed in anhydrous THF ultrasonically, added dropwise into the DRPU reaction liquid and mechanically stirred for 10 min. During mixing, a portion of THF was removed under reduced pressure to maintain the mixture's optimal viscosity. Finally, the mixture was transferred to a polytetrafluoroethylene (PTFE) mold, and the remaining THF was evaporated to obtain DRPUs/f_3-Al_2O_3.

3.4 Characterizations

Number average molecular weight (M_n), weight average molecular weight (M_w), and the polydispersity index (PDI) of prepolymer were determined by gel permeation chromatography (GPC, LC-20ADXR), with polystyrene as the standard sample and tetrahydrofuran as the eluent at a flow rate of 1 mL min^{-1}.

Fourier transform infrared (FT-IR) spectra of raw materials and DRPUs were obtained by an FT-IR instrument (Nicolet iS50, Thermo Fisher Scientific, USA) within the wavelength range of 4000 to 600 cm^{-1} at a resolution of 4 cm^{-1}. Proton nuclear magnetic resonance (^{1}H NMR) spectra were obtained by an Avance III HD 400 MHz spectrometer (Bruker, Switzerland) at an ambient temperature using deuterated dimethyl sulfoxide-d_6 (DMSO-d_6) as the solvent and tetramethylsilane (TMS) as the internal standard. X-ray diffraction (XRD) was performed using a diffractometer (D8, Bruker, Germany) within a range of 5–90°. The lap-shear test was performed using a universal testing machine (MTS E44.304 tensile testing machine) at a strain rate of 10 mm min^{-1} at room temperature. Three specimens were tested per sample, and the averaged results were reported. A

differential scanning calorimeter (DSC 3, METTLER TOLEDO, Switzerland) was used to observe the T_g of DRPUs under a nitrogen atmosphere. Samples were kept at −70 °C for 10 min and then heated from −70 °C to 80 °C at a rate of 10 °C min^{-1}. The thermal stabilities of DRPUs were determined *via* thermogravimetric analysis (TGA2, METTLER TOLEDO, Switzerland), and the samples were heated from 30 °C to 600 °C under an N_2 atmosphere at a heating rate of 10 °C min^{-1}. A KY-3201-A20T powder press machine (Dongguan Kaiyan Machinery Technology Co. Ltd, China) was used to prepare the polymer sheets (80 mm × 90 mm × 1 mm) for testing recyclability. Samples were preheated and hot pressed at 110 °C for 10 min under 15 MPa, followed by cold pressing to obtain sheets. Mechanical testing was carried out on an MTS E44.304 tensile testing machine (MTS, USA) at a crosshead speed of 50 mm min^{-1} and a temperature of 25 °C. Each sample was tested three times, and the results were averaged to get the mean value. The thermal conductivity was tested by a Hot Disk (TPS3000, Sweden) at a temperature of 25 °C.

4 Conclusions

In summary, DRPUs with high molecular weights were successfully synthesized using PTMEG, IPDI, TEA and a self-made chain extender DABF. Among a series of DRPUs, $DRPU_{0.52}$ demonstrated the optimal mechanical and thermal comprehensive performances, achieving a tensile strength of 35.8 MPa, an elongation at break of 714%, a toughness of 146.07 MJ m^{-3} and a $T_{d,5\%}$ of 264.8 °C. Additionally, the lap-shear strength of $DRPU_{0.52}$ was about 3.3 MPa, which was retained at 3.0 MPa after 5 recycles. $DRPU_{0.52}$ also displayed excellent self-healing properties, recovering 87% of its original mechanical properties after the self-healing process. To enhance thermal conductivity, Al_2O_3 modified with PDA (f_3-Al_2O_3) was incorporated into the matrix as a filler. $DRPU_{0.52}$/f_3-Al_2O_3 exhibited a progressive increase in thermal conductivity, with $DRPU_{0.52}$/80% f_3-Al_2O_3 achieving the highest thermal conductivity of 0.6329 W m^{-1} K^{-1}, which was 344.8% higher than that of original $DRPU_{0.52}$. These results suggest that DRPUs hold great promise as a matrix of TIMs, offering reliable and durable interfacial thermal transport properties.

Conflicts of interest

There are no conflicts to declare.

Data availability

The data that support the findings of this article can be obtained directly from the authors upon request.

Supplementary information (SI): additional synthesis and characterization of DABF, stability tests, stress–strain curves, polarized optical micrographs and healing efficiency of DRPUs. See DOI: https://doi.org/10.1039/d6ra00787b.

Acknowledgements

This work was supported by the Industrial-University Cooperation Project of Jiangsu Province (BY2020441).

References

1 M. C. K. Swamy and Satyanarayan, A Review of the Performance and Characterization of Conventional and Promising Thermal Interface Materials for Electronic Package Applications, *J. Electron. Mater.*, 2019, **48**, 7623–7634.
2 H. Y. Niu, Y. J. Ren, H. C. Guo, K. Małycha, K. Orzechowski and S. L. Bai, Recent progress on thermally conductive and electrical insulating rubber composites: design, processing and applications, *Compos. Commun.*, 2020, **22**, 100430.
3 C. G. Zhao, Y. F. Li, Y. C. Liu, H. Q. Xie and W. Yu, A critical review of the preparation strategies of thermally conductive and electrically insulating polymeric materials and their applications in heat dissipation of electronic devices, *Adv. Compos. Hybrid Mater.*, 2022, **6**, 27.
4 M. A. Alim, M. Z. Abdullah, M. S. A. Aziz, R. Kamarudin and P. Gunnasegaran, Recent advances on thermally conductive adhesive in electronic packaging: a review, *Polymers*, 2021, **13**, 3337.
5 B. J. Wei, W. M. Luo, J. Y. Du, Y. F. Ding, Y. J. Guo, G. M. Zhu, Y. Zhu and B. W. Li, Thermal interface materials: from fundamental research to applications, *SusMat*, 2024, **4**, 239.
6 X. F. Xu, J. Chen, J. Zhou and B. W. Li, Thermal conductivity of polymers and their nanocomposites, *Adv. Mater.*, 2018, **30**, 1705544.
7 M. Abbas, A. A. Septevani, F. Yurid, A. Joshi, M. Gupta, S. M. Rangappa, G. M. Madhu, M. Sriariyanun, S. Siengchin and P. Baranitharan, Thermal interface polymer-based composites materials: a critical review, *Multiscale Multidiscip. Model. Exp. Des*, 2025, **8**, 191.
8 P. P. Zhao, P. Lu, Z. Y. Zhao, S. W. Chen, X. Y. Li, C. Deng and Y. Z. Wang, Aromatic Schiff base-based polymeric phase change materials for safe, leak-free, and efficient thermal energy management, *Chem. Eng. J.*, 2022, **437**, 135461.
9 Y. J. Xue, J. Y. Lin, T. Wan, Y. L. Luo, Z. W. Ma, Y. H. Zhou, B. T. Tuten, M. Zhang, X. Y. Tao and P. G. Song, Stretchable, ultratough, and intrinsically self-extinguishing elastomers with desirable recyclability, *Adv. Sci.*, 2023, **10**, 2207268.
10 X. D. Kong, Y. P. Chen, R. J. Yang, Y. D. Wang, Z. B. Zhang, M. H. Li, H. X. Chen, L. H. Li, P. Gong, J. X. Zhang, K. Xu, Y. Cao, T. Cai, Q. W. Yan, W. Dai, X. F. Wu, C. T. Lin, K. Nishimura, Z. B. Pan, N. Jiang and J. H. Yu, Large-scale production of boron nitride nanosheets for flexible thermal interface materials with highly thermally conductive and low dielectric constant, *Composites, Part B*, 2024, **271**, 111164.
11 P. Nellepalli, T. Patel and J. K. Oh, Dynamic covalent polyurethane network materials: synthesis and self-healability, *Macromol. Rapid Commun.*, 2021, **42**, 2100391.

12 Y. L. Fang, J. H. Xu, F. Gao, X. S. Du, Z. L. Du, X. Cheng and H. B. Wang, Self-healable and recyclable polyurethane-polyaniline hydrogel toward flexible strain sensor, *Composites, Part B*, 2021, **219**, 108965.

13 Z. Q. Li, Y. L. Zhu, W. W. Niu, X. Yang, Z. Y. Jiang, Z. Y. Lu, X. K. Liu and J. Q. Sun, Healable and recyclable elastomers with record-high mechanical robustness, unprecedented crack tolerance, and superhigh elastic restorability, *Adv. Mater.*, 2021, **33**, 2101498.

14 Y. A. Zhang, P. Wu, Y. Meng, R. W. Lu, S. F. Zhang and B. T. Tang, Flexible phase change films with enhanced thermal conductivity and low electrical conductivity for thermal management, *Chem. Eng. J.*, 2023, **464**, 142650.

15 Y. C. Jia, J. J. Qian, S. Y. Hao, S. J. Zhang, F. C. Wei, H. J. Zheng, Y. L. Li, J. W. Song and Z. W. Zhao, New prospects arising from dynamically crosslinked polymers: reprogramming their properties, *Adv. Mater.*, 2024, **36**, 2313164.

16 Z. Shi, J. Kang and L. Zhang, Water-enabled room-temperature self-healing and recyclable polyurea materials with super-strong strength, toughness, and large stretchability, *ACS Appl. Mater. Interfaces*, 2020, **12**, 23484–23493.

17 X. T. Zhang, S. J. Wang, Z. K. Jiang, Y. Li and X. L. Jing, Boronic ester based vitrimers with enhanced stability via internal boron-nitrogen coordination, *J. Am. Chem. Soc.*, 2020, **142**, 21852–21860.

18 J. Xie, L. Fan, D. Yao, F. Su, Z. Mu and Y. Zheng, Ultra-robust, self-healable and recyclable polyurethane elastomer via a combination of hydrogen bonds, dynamic chemistry, and microphase separation, *Mater. Today Chem.*, 2022, **23**, 100708.

19 Z. Y. Wang, H. B. Liang, H. T. Yang, L. Xiong, J. P. Zhou, S. M. Huang, C. H. Zhao, J. Zhong and X. F. Fan, UV-curable self-healing polyurethane coating based on thiol-ene and Diels-Alder double click reactions, *Prog. Org. Coat.*, 2019, **137**, 105282.

20 Z. Q. Wu, J. Dong, H. Guo, R. Shang, X. Z. Qin, Y. F. Xia, X. T. Li, X. Zhao, C. C. Ji and Q. H. Zhang, Robust, self-healing, and multi-use poly(urethane-urea-imide) elastomer as a durable adhesive for thermal interface materials, *Small*, 2024, **20**, 2401815.

21 M. Li, R. C. Zhang, X. H. Li, Q. Wu, T. H. Chen and P. C. Sun, High-performance recyclable cross-linked polyurethane with orthogonal dynamic bonds: the molecular design, microstructures, and macroscopic properties, *Polymer*, 2018, **148**, 127–137.

22 X. L. Lu, G. X. Fei and H. S. Xia, Ultrasound healable shape memory dynamic polymers, *J. Mater. Chem. A*, 2014, **2**, 16051–16060.

23 K. W. Zheng, Y. Z. Tian, M. J. Fan, J. Y. Zhang and J. Cheng, Recyclable, shape-memory, and self-healing soy oil-based polyurethane crosslinked by a thermoreversible Diels-Alder reaction, *J. Appl. Polym. Sci.*, 2018, **135**, 46049.

24 D. B. Zhu, C. Y. Guo, H. C. Liu, J. F. Ye, H. R. Chen, J. B. Zhang, Y. H. Liu and L. B. Feng, Thermo-reversible DA bonds-based polyurethanes with both excellent comprehensive mechanical property and remarkable room temperature self-healing capability, *Colloids Surf., A*, 2025, **711**, 136398.

25 K. Ku and H. Yeo, Molecular orientation and thermal conductivity in liquid crystalline epoxy resins by anionic ring-opening polymerization, *Ind. Eng. Chem. Res.*, 2024, **63**(46), 20059–20064.

26 I. L. Williams, N. Barua, L. Menges, G. Barrera, V. Vasudevan and T. Hutter, Thermally controlled benzene sorption using pdms-infused macroporous silicon matrices, *ACS Appl. Mater. Interfaces*, 2026, **18**(4), 7328–7340.

27 R. H. Wang, H. H. Zhao, T. K. Yue, S. K. Yang and J. Liu, Understanding thermal conductivity of polymer composites with hybrid fillers: a molecular dynamics simulation study, *ACS Appl. Polym. Mater.*, 2025, **7**(2), 878–888.

28 M. J. Zhang, X. Huang, Y. Q. Wang, C. Y. Zhang and Y. X. Ni, Advances in simulations of thermal transport in carbon nanotubes and graphene reinforced polymer composites: from microscopic, mesoscopic to macroscopic, *Polym. Compos.*, 2025, **0**, 1–25.

29 K. Xu, Y. H. Zhou, R. J. Yang, Z. J. Zhao, C. Q. Gao, Y. R. Wang, G. Huang, Y. X. Ni, X. Huang, C. Y. Zhang and Y. Q. Wang, Magnetic alignment of carbon nanotubes in polymers for enhanced thermal conductivity, *Nanoscale*, 2025, **17**(48), 28185–28194.

30 W. G. Zhou, M. Q. Sun, L. Yang, J. Fang, J. Q. Zhu, C. X. Yan, X. J. Liu, X. Han and J. G. Gao, Construction of a controllable dual-channel structure of Al_2O_3 and boron nitride within cellulose nanofiber composite films to improve through-plane thermal conductivity, *Polymer*, 2025, **330**, 128520.

31 C. P. Yu, J. Zhang, W. Tian, X. D. Fan and Y. G. Yao, Polymer composites based on hexagonal boron nitride and their application in thermally conductive composites, *RSC Adv.*, 2018, **8**, 21948.

32 Y. Chen, H. G. Zhang, J. Chen, Y. T. Guo, P. K. Jiang, F. Gao, H. Bao and X. Y. Huang, Thermally Conductive but electrically insulating polybenzazole nanofiber/boron nitride nanosheets nanocomposite paper for heat dissipation of 5g base stations and transformers, *ACS Nano*, 2022, **16**, 14323–14333.

33 T. T. Truong, H. T. Nguyen, M. N. Phan and L. T. Nguyen, Study of Diels-Alder reactions between furan and maleimide model compounds and the preparation of a healable thermo-reversible polyurethane, *J. Polym. Sci., Part A:Polym. Chem.*, 2018, **56**, 1806–1814.

34 K. Xiong, T. T. Yang, Z. P. Sun, C. Ma, J. T. Wang, X. Ge, W. M. Qiao and L. C. Ling, Modified graphene film powder scraps for re-preparation of highly thermally conductive flexible graphite heat spreaders, *Carbon*, 2014, **219**, 118827.

35 R. K. Du, L. He, P. Li and G. Z. Zhao, Polydopamine-modified al_2o_3/polyurethane composites with largely improved thermal and mechanical properties, *Materials*, 2020, **13**, 1772.